A Cloud-Edge Collaboration Framework for Cancer Survival Prediction to Develop Medical Consumer Electronic Devices

Suixue Wang, Zhigao Zheng, *Member, IEEE*, Xinghong Wang, Qingchen Zhang, *Senior Member, IEEE*, and Zhuo Liu

***Abstract*—Consumer electronics, together with artificial intelligence technology, are being widely applied in the medical field, aiding medical data collecting, health monitoring, disease diagnosis, and survival prediction. Training an effective and robust medical artificial intelligence model for cancer survival prediction deployed in consumer electronic devices requires a large amount of high-quality annotated data. However, due to limitations in computing resources and energy, it is impractical to train artificial intelligence models on large-scale medical data directly in the cloud. To address the above problem, we propose a cloud-edge collaboration framework to develop medical electronic devices for cancer survival prediction. The framework trains local models on edge medical electronic devices and aggregates the model weights on the cloud server. Furthermore, when transmitting model weights between cloud and edge, we introduce differential privacy technology to ensure security concerns. We evaluate our proposed cloud-edge collaboration framework on two cancer datasets from The Cancer Genome Atlas (TCGA). Experimental results demonstrate that our cloud-edge collaboration framework is highly effective in both survival prediction performance and patient privacy preservation, with the potential to develop medical consumer electronics.**

***Index Terms*—Cloud-edge collaboration, medical consumer electronics, large-scale medical data, differential privacy, survival prediction.**

I. Introduction

CONSUMER electronics, combined with medical technology, has greatly promoted the development of medical electronics, garnering increasing attention in recent years [1], [2]. Medical electronics, as an essential component of consumer electronics, have a significant impact in the field of modern medicine [3]. They offer important assistance in health monitoring, disease diagnosis, and survival prediction through collecting, analyzing, and transmitting large-scale medical data such as X-rays, CT, MRI, histopathological images, and multi-omics data [4]. For instance, medical electronic devices such as glucose monitors and electrocardiographs facilitate real-time patient physiological data monitoring, aiding doctors' comprehension of the patient's health status [5]. Additionally, imaging devices such as CT scans and MRIs offer high-resolution medical images, furnishing clinicians with precise diagnostic information [6].

The success of medical consumer electronics in the medical field is primarily attributed to artificial intelligence (AI) technology and large-scale medical data. Specifically, we typically utilize a large amount of high-quality annotated medical data, (*e.g.,*medical history, clinical notes, laboratory results, radiomics, pathological images, and multi-omics data.) [7] to develop a reliable and powerful AI model tailored for healthcare applications. This facilitates medical electronics to improve the precision of health monitoring, computer-aided diagnosis, and survival prognosis. However, due to the scarcity of annotated data, long-term follow-up, data collection, and data management require considerable time and resources. Hence, it is difficult for a single medical device to collect such large-scale medical data. Although data centralization-based approaches with data sharing can effectively solve the problem of large-scale medical data collecting and improve AI model performance, there are still two issues that need to be solved: 1) Firstly, training AI models on large-scale medical data directly in the cloud is impractical due to constraints in computational resources and energy. Therefore, careful thinking and design are needed on how to combine edge computing with cloud computing to alleviate the problem of computing power for training medical AI models, where edge computing is a burgeoning computing paradigm that involves various networks and devices around or near the user. In this paradigm, edge nodes can deal with data close to their source, enabling the processing of large-scale data in real time. 2) Secondly, the transmission and sharing of medical data between edge medical electronic devices and a cloud server may be at risk of cyber-attacks [8], leading to the leakage of patients' private information and posing serious

Manuscript received 22 March 2024; revised 1 May 2024; accepted 5 June 2024. Date of publication 13 June 2024; date of current version 11 December 2024. This work was supported by the National Natural Science Foundation of China under Grant 62162023 and Grant KYQD(ZR)-21079. *(Corresponding author: Zhuo Liu.)*

Suixue Wang is with the School of Information and Communication Engineering, Hainan University, Haikou 570228, China (e-mail: wangsuixue@hainanu.edu.cn).

Zhigao Zheng is with the School of Computer Science, Wuhan University, Wuhan 430072, China (e-mail: zhengzhigao@ieee.org).

Xinghong Wang is with the Department of Clinical Laboratory Diagnostics, First Affiliated Hospital of Hainan Medical College, Haikou 570102, China (e-mail: Wxh20230606@163.com).

Qingchen Zhang is with the School of Computer Science and Technology, Hainan University, Haikou 570228, China (e-mail: zhangqingchen@hainanu.edu.cn).

Zhuo Liu is with the Department of Respiratory and Critical Care Medicine, First Affiliated Hospital of Dalian Medical University, Dalian 116000, China (e-mail: lzhuo0310@126.com).

Digital Object Identifier 10.1109/TCE.2024.3413732

risks such as discrimination, extortion, and harm. Therefore, it is vital to develop an AI approach deployed in medical electronic devices to address computing power and privacy preservation challenges, while enhancing the precision of AI model performance.

To address the above problem, we propose a cloud-edge collaboration framework to develop medical consumer electronic devices for cancer survival prediction. Specifically, the framework first transfers medical data from near-end edge devices, including histopathology images, multi-omics data, survival time, and survival status, to an edge server via a local area network (LAN). Then, local medical AI models are trained by introducing an edge computing paradigm [28] on the edge server. Subsequently, the local model weights are transmitted to the cloud server by leveraging a differential privacy technique [9]. In the cloud, the average federated learning technique [10] is introduced to aggregate the model weights from various edge nodes and generate a global model. Finally, the global model is inverted back to the edge nodes for ongoing training or inference of survival prediction. In the local model structure, we utilize a Vision Transformer (ViT) [11] and a cross-attention mechanism [12] to comprehensively fuse histopathology images and multi-omics modalities. We evaluate our proposed cloud-edge collaborative framework on two cancer datasets, breast invasive carcinoma (BRCA) and lower grade glioma (LGG), from The Cancer Genome Atlas (TCGA) [13]. The experimental results highlight the effectiveness of our cloud-edge collaboration framework in survival prediction performance and patient privacy preservation. Furthermore, this framework holds promising potential for the development of medical consumer electronics.

In summary, our contributions can be outlined as follows:

1) We propose a cloud-edge collaboration framework to develop medical consumer electronics devices for cancer survival prediction.
2) We introduce federated learning into the framework, enabling medical consumer electronics devices to process large-scale medical data in real-time.
3) We incorporate differential privacy into the weights of the survival prediction models before transmitting the model weights between edge nodes and a cloud center, to ensure patient data security.

The remainder of this study is structured as follows. Section II surveys the relevant collaboration frameworks used in medical electronic devices. Section III presents the proposed cloud-edge collaboration framework in two primary components. Section IV conducts experiments on two cancer datasets to assess the efficacy of the proposed framework. Lastly, Section V offers the conclusion of this paper.

II. Related Work

With the continuous expansion of medical consumer electronic devices, data centralization enhances the reliability of health monitoring and improves the accuracy of disease diagnosis. In recent years, the data centralization-based multi-center collaboration methods have shown remarkable success in healthcare data aggregation and transmission [14]. For instance, Imakura and Sakurai [15] introduced a collaborative analysis framework for distributed datasets. This framework remained the original datasets and models distributed across multiple institutions by employing centralized machine learning [29]. Yang et al. [16] designed a solution to protect the privacy of medical records in a cloud computing environment, using attribute-based classification and vertical partitioning of medical datasets to meet the privacy requirements of different parts. Albarqouni et al. [17] introduced a novel concept by integrating a crowdsourcing layer that enables direct crowd participation in data aggregation, thus incorporating them into the convolutional neural network learning process. Although sharing data among multiple medical devices can improve the performance of models by centralizing data, it also poses a risk of exposing patients' private information to cyber threats.

Federated learning (FL) is a crucial advancement of multi-center collaboration in machine learning. It effectively reduces the risk of data leakage by sharing model weights/gradients among multi-institutions without sharing the original data directly [30], [31]. More recently, several studies have achieved outstanding results in FL for healthcare. For example, Zhang et al. [19] presented an innovative framework called SSL-FTBT, which implements self-supervised federated learning based on pseudo-data and aims to enhance the generalization of computer-aided diagnosis models and diagnostic accuracy. Choudhury et al. [20] introduced a federated learning framework that offers two tiers of privacy protection for constructing global models using distributed health data stored locally across various sites. Moreover, the studies of cloud-edge collaboration have demonstrated outstanding success in multi-center collaboration. Ding et al. [21] proposed a cloud-edge collaboration framework with fast response and high accuracy characteristics by implementing a shallow model on edge servers and a deep model on cloud servers.

In the past few years, researchers have shown significant interest in deep learning-based multimodal models integrating histopathological images and multi-omics data for cancer survival prediction [22], [23]. For instance, Wang et al. [12] introduced a hierarchical aggregation strategy and cross-attention mechanism to the multimodal survival model, proposing a hierarchy-based approach to combine multi-omics data and histopathological images. Wu et al. [24] presented a cross-aligned multimodal representation learning approach to generate two distinct types of representations: modality-invariant and modality-specific. This approach was shown to improve the accuracy of cancer survival prediction. Nonetheless, few studies have investigated the employment of multimodal survival models in federated learning and cloud-edge collaboration frameworks. Lu et al. [25] introduced the differential privacy and weakly-supervised attention mechanism to multiple instance learning, proposing a histopathological image-based privacy-preserving federated learning framework for cancer subtyping and survival prediction. Wang et al. [26] presented a multimodal-based vertical federated learning framework fusing multi-omics data sourced from various institutions for cancer survival prediction. However, the above approaches were limited to supporting unimodal data as input.

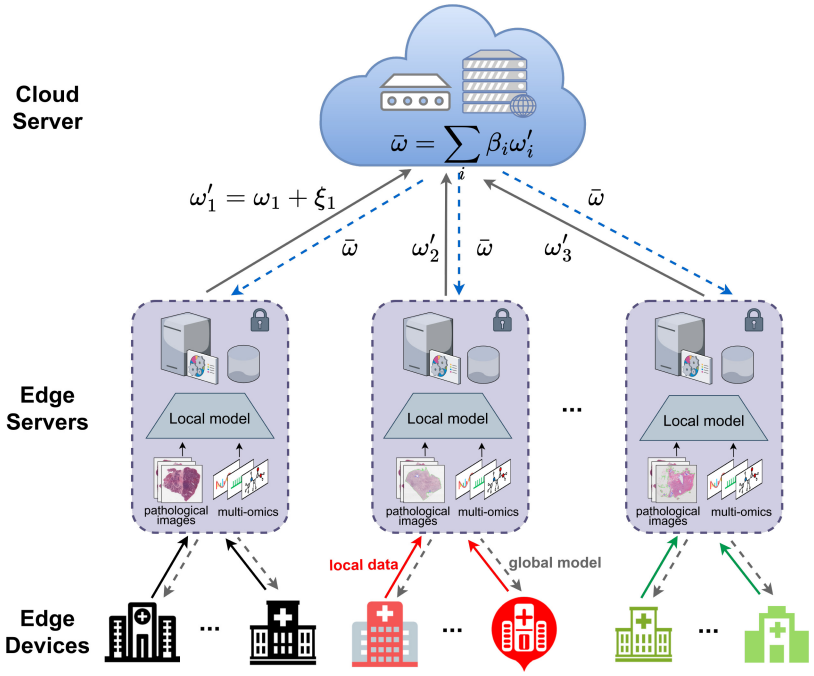

Fig. 1. The cloud-edge collaboration framework using federated learning and differential privacy.

III. Method

In this section, we will formulate our proposed framework in two primary parts: the cloud-edge collaboration framework and the local multimodal model fusing histopathological images and multi-omics data. The details of our framework are described in the subsequent subsections.

A. The Cloud-Edge Collaboration Framework

The overview of our proposed cloud-edge collaboration framework is shown in Fig. 1. The framework is structured as a pyramid with three layers: the edge device at the bottom, the edge server in the middle, and the cloud server at the top. The edge device layer corresponds to fundamental medical facilities like clinics and small hospitals, tasked with initial data collection and AI model inference. The edge server layer pertains to larger medical centers such as general hospitals and research institutions, often overseeing multiple associated small hospitals for local model training. Finally, the cloud server, situated in the cloud center, plays a vital role in aggregating model parameters from edge servers for comprehensive analysis.

Assuming that there are N medical institutions (edge devices) corresponding to the N edge servers, which are denoted as $\mathbf{S}_1, \ldots, \mathbf{S}_N$. Each institution $\mathbf{S}_n$ has a local dataset $\mathcal{D}_n$ collected from corresponding edge devices, where $\mathcal{D}_n$ consists of histopathological images $\mathbf{I}_n$, multi-omics $\mathbf{o}_n$, survival time T_n, and survival status E_n. When training the m-th round of the local model, the weights of the local model are updated by:

$$\omega_n^m \leftarrow \mathit{LocalUpdated}\left(\mathcal{L}_n; \omega_n^m\right) \tag{1}$$

where ω is the model weights, $\mathit{LocalUpdated}(\cdot)$ denotes the process of optimizing local model training, and $\mathcal{L}_n$ refers to the loss function of local survival model.

The cloud server aggregates the model weights received from N edge servers using the average federated learning method, generating global model weights for the m-th round, which is written as:

$$\bar{\omega}^m = \frac{1}{N} \sum_{n=0}^{N-1} \omega_n^m \tag{2}$$

Subsequently, the global model weights $\bar{\omega}^m$ are transmitted back to all the edge servers for the next round of local model training. When the iteration reaches a set number of rounds M, the model training is terminated and the last round of global model weights $\bar{\omega}^M$ are passed back to all edge devices for deployment and online inference.

To protect the privacy of model weights during the collaboration between the cloud server and edge server, the (ϵ, δ)-differential privacy is introduced into our cloud-edge collaboration framework. (ϵ, δ)-differential privacy aims to protect individual privacy by ensuring that the output of a computation does not change significantly when one data point is added or removed from the dataset. Formally, given privacy parameters $\epsilon \geq 0$ and $\delta \in [0, 1]$, a randomized algorithm $\mathcal{F}$ satisfies (ϵ,δ)-differential privacy if for all pairs of neighboring datasets $\mathcal{D}$ and $\mathcal{D}'$ that differ in only one data point, and for all measurable sets C in the output space:

$$\Pr[\mathcal{F}(\mathcal{D}) \in C] \leq e^{\epsilon} \Pr\left[\mathcal{F}\left(\mathcal{D}'\right) \in C\right] + \delta \tag{3}$$

where ϵ and δ are privacy parameters. A smaller ϵ indicates stricter privacy protection. δ represents the probability that the privacy guarantee might be breached.

The Gaussian mechanism is widely used to achieve (ϵ,δ)-differential privacy by adding Gaussian noise to query results, ensuring information privacy. To compute the mean and variance of Gaussian noise efficiently, we can utilize the properties of Gaussian distribution. The mean of Gaussian

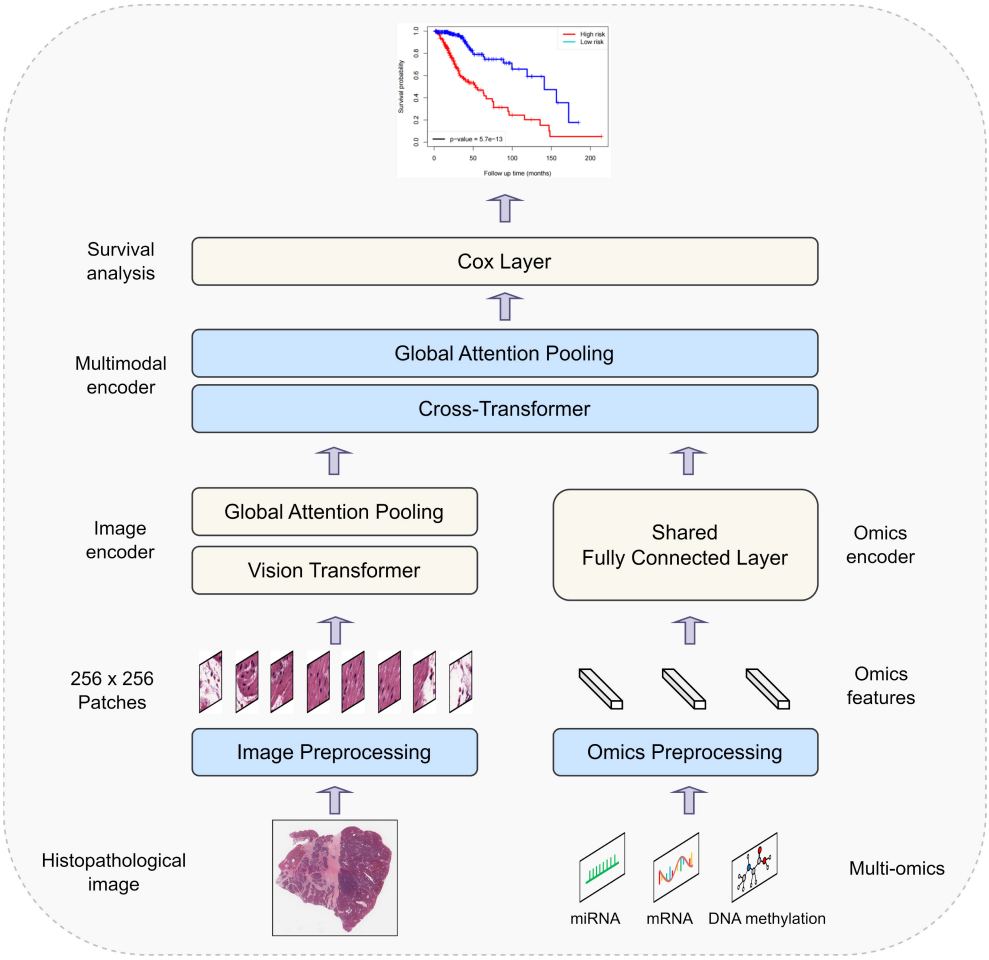

Fig. 2. The local multimodal model fusing histopathological images and multi-omics.

noise is typically set to zero. For arbitrary $\epsilon \in (0, 1)$, the standard deviation derived from [27] is written as:

$$\sigma \geq \Delta_2(\mathcal{F})\sqrt{2\ln(1.25/\delta)}/\epsilon \tag{4}$$

where $\Delta_2(\mathcal{F})$ is the ℓ_2-sensitivity of the function $\mathcal{F}$, which is computed as follows:

$$\Delta_2(\mathcal{F}) = \max_{\|\mathcal{D}-\mathcal{D}'\|_1=1} \left\|\mathcal{F}(\mathcal{D}) - \mathcal{F}(\mathcal{D}')\right\|_2 \tag{5}$$

Due to the complexity of our local model consisting of multiple modules and many layers with trainable weights, it is intractable to calculate the $\Delta_2(\mathcal{F})$ directly. Hence, we simplify the formula of the standard deviation by setting $\Delta_2(\mathcal{F})$ to 1 and ϵ to 1. As a result, the distribution of Gaussian noise can be written as:

$$\xi \sim \mathcal{N}(0, 2\ln(1.25/\delta)) \tag{6}$$

When adding the Gaussian noise to our framework, the Eq. (2) is updated as:

$$\bar{\omega}^m = \frac{1}{N}\sum_{n=0}^{N-1}\left(\omega_n^m + \xi_n^m\right) \tag{7}$$

B. Local Multimodal Model Fusing WSIs and Multi-Omics Data

In this section, we outline a comprehensive description of our local multimodal model that fuses histopathological images and multi-omics data for cancer survival analysis, as illustrated in Fig. 2.

Given that $\mathbf{I}_n = \{\mathbf{I}_{n,l}\}_{l=1}^{L} \in \mathbb{R}^{L\times(256\times256\times3)}$ and $\mathbf{o}_n \in \mathbb{R}^{3\times300}$ are the preprocessing results of histopathological images and multi-omics, respectively, where L is the number of image patches with 256×256 pixels. Each image patch $\mathbf{I}_{n,l}$ is fed into a pre-trained Vision Transformer (image encoder), which is proposed by Dosovitskiy et al. [11] and pre-trained using histopathological image patches of sizes 256×256 by our previous work [12], for obtaining the image representations:

$$\mathbf{x}_{n-im} = AttnPool\Big(ViT\Big(\{\mathbf{I}_{n,l}\}_{l=1}^{L}\Big)\Big), \mathbf{x}_{n-im} \in \mathbb{R}^{L\times d} \tag{8}$$

where $ViT(\cdot)$ is the pre-trained ViT model, $AttnPool(\cdot)$ signifies the global attention pooling operation, and d is the dimension of ViT outputs.

Moreover, a shared fully connected layer (omics encoder) is employed to learn the omics presentations, while aligning the dimension of the multi-omics data with the dimensions of the ViT encoder outputs:

$$\mathbf{x}_{n-om} = MLP(\mathbf{o}_n), \mathbf{x}_{n-om} \in \mathbb{R}^{3\times d} \tag{9}$$

Subsequently, we present a cross-attention-based multimodal encoder, namely Cross-Transformer, for integrating the histopathological images and multi-omics data. The integrative processes are written as:

$$\begin{aligned}\mathbf{x}_{n-fuse} &= CrossAttn\left(\mathbf{w}_q\mathbf{x}_{n-om}, \mathbf{w}_k\mathbf{x}_{n-im}, \mathbf{w}_v\mathbf{x}_{n-im}\right) \\ &= Softmax\left(\frac{\mathbf{w}_q\mathbf{x}_{n-om}\mathbf{x}_{n-im}^T\mathbf{w}_k^T}{\sqrt{d}}\right)\mathbf{w}_v\mathbf{x}_{n-im}\end{aligned} \tag{10}$$

$$\mathbf{x}_n = AttnPool\left(Trans\left(\left[\mathbf{x}_{n-fuse} \oplus \mathbf{x}_{n-om}\right]\right)\right) \tag{11}$$

where $\mathbf{w}_v, \mathbf{w}_k, \mathbf{w}_q \in \mathbb{R}^{d\times d}$ indicate learnable weights multiplied by the values $\mathbf{x}_{n-im}$, keys $\mathbf{x}_{n-im}$, and queries $\mathbf{x}_{n-om}$, respectively. $Trans(\cdot)$ is the standard Transformer with several blocks, $\oplus$ is the concatenation operation, and $\mathbf{x}_n$ is the final multimodal representation.

Lastly, the final representations $\mathbf{x}_n$ integrating multimodal data are fed into a Cox layer, which is implemented by a fully-connected network, for computing the survival risk score. During survival prediction, the average negative log partial likelihood [12] is adopted to combine the survival risk, survival time T_n, and survival status E_n, as the objective function of our local multimodal model, which is denoted as:

$$\begin{aligned}&\mathcal{L}\ (\mathbf{x}_n, E_n, T_n) = \\ &-\frac{1}{n_E}\sum_{i:E_{n,i}=1}\left(\boldsymbol{\alpha}\mathbf{x}_n^{(i)} - \log\sum_{j:T_{n,j}>T_{n,i}} e^{\boldsymbol{\alpha}\mathbf{x}_n^{(j)}}\right)\end{aligned} \tag{12}$$

where α denotes the learnable weights in the fully-connected linear layer, and the linear layer $\boldsymbol{\alpha}\mathbf{x}_n^{(i)}$ is utilized for predicting the survival risk score. n_E represents the quantity of uncensored samples.

C. Implementation Details

Herein, Algorithm 1 illustrates our framework for collaboratively training a multimodal survival model between a cloud server and multiple edge servers. The cloud-edge collaboration framework is developed using PyTorch and runs on a workstation featuring three NVIDIA A100 GPUs, each with a capacity of 80 GB. The structure of the ViT-based image encoder is kept the same as the original ViT base model. The standard Transformer used in the multimodal encoder consists of 3 blocks and 12 heads. The Adam optimization with a learning rate of 5e-4 and a weight decay of 1e-3 is used for training the local model. Since the histopathological images have various sizes of patches, the batch size is configured as 1 with 60 steps of gradient accumulation. The training epoch is set to 80.

Moreover, the interaction between multiple edge nodes and the cloud center for model parameters is implemented by using a rough and straightforward strategy. Initially, we execute a Python script for the cloud center and three analogous Python scripts with different datasets for three edge nodes. Subsequently, edge scripts train the local model, save a model checkpoint to the local disk, and then enter a loop to await the global model checkpoint. Next, the cloud script checks whether all local model checkpoints at the current round are ready. Once confirmed, the cloud script aggregates them and saves the checkpoint to the local disk as the global model weight. After that, edge scripts reload the global model weight and continue training the model.

Algorithm 1 The Cloud-Edge Collaboration Framework

INPUT: Number of edge servers N, number of training epochs M, privacy parameter δ for generating Gaussian noise, and local datasets $\mathcal{D} = \{[\mathbf{I}_n, \mathbf{o}_n, T_n, E_n]\}_{n=0}^{N-1}$.
OUTPUT: The final global weights $\bar{\omega}^{M-1}$.
TRAIN:
initialize all model weights $\bar{\omega}^0, \omega_0^0, \omega_1^0, \ldots, \omega_{N-1}^0$
For $m = 0, 1, \ldots, M-1$ **do**
  For $n = 0, 1, \ldots, N-1$ **in parallel do**
    $\mathbf{x}_n^m = \mathcal{F}(\mathbf{I}_n, \mathbf{o}_n; \omega_n^m)$
    $\omega_n^m \leftarrow LocalUpdated(\mathcal{L}(\mathbf{x}_n^m, E_n, T_n); \omega_n^m)$
  end for
  $\bar{\omega}^m = \frac{1}{N}\sum_{n=0}^{N-1}(\omega_n^m + \xi_n^m)$
  For $n = 0, 1, \ldots, N-1$ **do**
    $\omega_n^{m+1} \leftarrow \bar{\omega}^m$
  end for
end for
Return $\bar{\omega}^{M-1}$

IV. EXPERIMENTS

In this section, we start by introducing the datasets and the preprocessing pipeline applied in this paper. Subsequently, we show the experimental results on multi-institutional multimodal data under various settings. Finally, we study the impact of model generalization and the frequency of model weight updates on performance.

A. Data Preprocessing

We conduct experiments on BRCA and LGG cancer datasets sourced from TCGA. Each patient sample consists of two modalities: histopathological images and multi-omics data. The multi-omics data comprises three types of omics: namely RNA-Seq, miRNA, and DNA methylation. We removed patient samples with missing data types to implement the local multimodal model. In addition, patients with a survival time of fewer than 30 days or lacking follow-up information were not included [12]. Finally, the sample sizes for BRCA and LGG were 724 and 451, respectively.

Following our previous work [12], the CLAM model [18] was applied to identify high-value regions within histopathological images and crop them into 256 × 256 patches. Moreover, the K-nearest neighbor interpolation, differential expression analysis, and random survival forest were introduced to select the top 300 important genes.

To simulate cloud-edge collaboration across multi-institutions (multiple edge nodes), we randomly divide the BRCA and LGG datasets into 3 non-overlapping, approximately equal-sized subsets to construct 3 different institutional sites, respectively. The data partitions are shown in Table I. Furthermore, the metric of concordance index

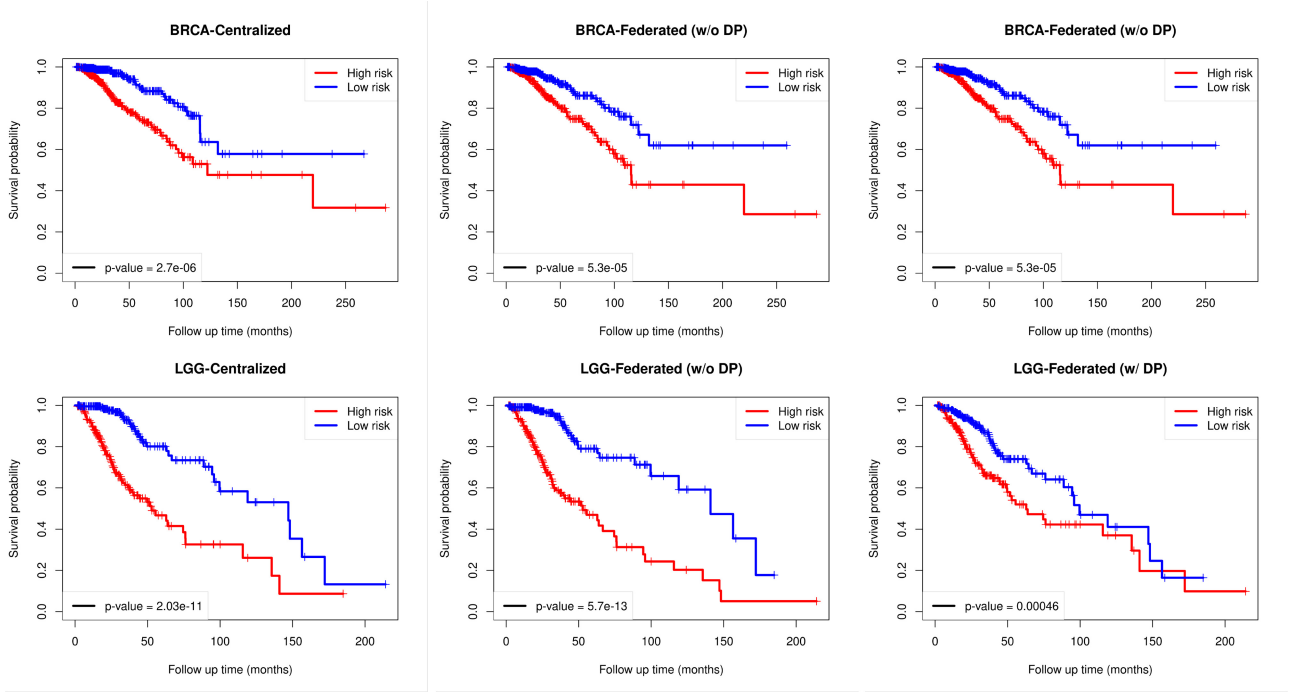

Fig. 3. Performance comparison of Centralized setting and our framework with Federated settings using Kaplan-Meier curves.

TABLE I
DATA PARTITIONS FOR CONSTRUCTING INSTITUTIONAL SITES

Node type	BRCA		LGG	
	Censored	Total	Censored	Total
Edge server 1	33	242	31	151
Edge server 2	28	241	46	150
Edge server 3	33	241	34	150
Total	94	724	111	451

TABLE II
CLOUD-EDGE SURVIVAL PREDICTION

Node type	BRCA	LGG
Edge server 1	0.628±0.068	0.823±0.031
Edge server 2	0.627±0.066	0.820±0.047
Edge server 3	0.566±0.052	0.821±0.028
Centralized	0.690±0.076	0.855±0.021
Federated (w/ DP)	0.671±0.063	0.840±0.043
Federated (w/o DP)	0.677±0.059	0.846±0.033

Note: The optimal and second-best results are highlighted in blue and red, respectively.

(C-index) with 5-fold cross-validation was utilized to evaluate the performance of cancer survival prediction.

B. Results on Multi-Institutional Multimodal Data

To verify the effectiveness of our proposed cloud-edge collaboration framework, we conduct experiments on multi-institutional multimodal data under the following settings:

1) Edge server 1/2/3: Models were trained solely on in-institution training data and evaluated using testing sets from all edge servers.
2) Centralized: Models were trained and evaluated using training and testing sets from all servers, respectively.
3) Federated (w/ DP): Our proposed cloud-edge collaboration framework with FL and DP.
4) Federated (w/o DP): Our proposed cloud-edge collaboration framework with FL, but without adding DP.

The experimental results are depicted in Table II. The Centralized setting obtained the highest C-index values in both the BRCA and LGG datasets, indicating that direct data aggregation is the most effective way to improve performance, but it is at the highest privacy risk. Moreover, the Federated (w/o DP) setting, our framework without DP, achieves suboptimal results, followed by the Federated (w/ DP) setting, our framework with DP. Compared to the Centralized and Federated settings, the survival prediction performance of the local model within any of the isolated institutional sites is relatively poor. The experimental results demonstrate that our framework effectively enhances the survival prediction performance without directly sharing data, safeguarding patient privacy. Furthermore, the Kaplan-Meier curves, along with their respective log-rank test p-values generated by Centralized and Federated settings, are illustrated in Fig. 3. Similarly, our framework with federated settings achieves comparable results to the framework with the centralized setting. In addition, the p-value of a cloud-edge collaboration framework increases when introducing differential privacy into the local multimodal model.

C. Study of Model Generalization

In this section, we examine the performance of breast cancer survival prediction within and among institutional data to evaluate the robustness and generalization of models corresponding to various settings. As displayed in

TABLE III
SURVIVAL PREDICTION PERFORMANCE TESTED ON INTRA VS. INTER-INSTITUTIONAL TEST DATA

	Edge server 1	Edge server 2	Edge server 3	Total
Edge server 1	0.601±0.048	0.643±0.028	0.619±0.053	0.628±0.068
Edge server 2	0.598±0.051	0.672±0.064	0.573±0.032	0.627±0.066
Edge server 3	0.592±0.034	0.563±0.045	0.527±0.064	0.566±0.052
Centralized	0.691±0.032	0.712±0.029	0.687±0.040	0.690±0.076
Federated (w/ DP)	0.673±0.041	0.685±0.055	0.623±0.023	0.671±0.063
Federated (w/o DP)	0.690±0.062	0.679±0.018	0.635±0.051	0.677±0.059

Note: The optimal and second-best results are highlighted in blue and red, respectively.

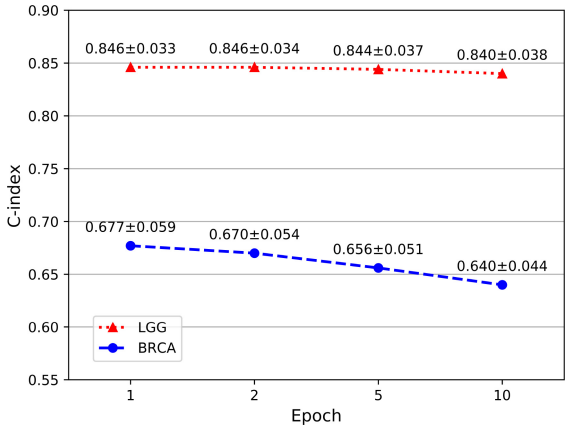

Fig. 4. The performance of cloud-edge collaboration framework for different communication pace.

Table III, undoubtedly, the Centralized setting achieves the best performance in any isolated institutional data set (inter-institution) and testing set from all institutions (intra-institution). Besides, our cloud-edge collaboration framework, including Federated (w/ DP) and Federated (w/o DP) settings, exhibits highly competitive performance against the settings in any isolated institution.

D. Study on the Frequency of Model Weight Updates

To explore how many training epochs to aggregate and update the model weights can achieve optimal performance, we investigate the impact of the frequency at which model weights are updated on the performance of survival prediction. We configured the aggregation and updating of model weights at intervals of 1, 2, 5, and 10 epochs, respectively. The performance of the survival prediction is illustrated in Fig. 4. It is evident that aggregating the weights of local models and updating them after each epoch is more suitable for our cloud-edge collaboration framework.

V. CONCLUSION

In this work, we propose a cloud-edge collaboration framework based on federated learning and differential privacy to develop medical consumer electronics devices for cancer survival prediction. The framework trains local medical AI models on a range of edge nodes and aggregates the model weights from various edge nodes on the cloud center. Moreover, the differential privacy technique is introduced into the survival prediction models before transmitting the model weights between edge nodes and a cloud center to safeguard patient data confidentiality. We evaluate the performance of our proposed cloud-edge collaboration framework on BRCA and LGG cancer datasets, which are sourced from TCGA. The experimental results demonstrate that our cloud-edge collaboration framework improves the accuracy of survival prediction models while safeguarding patient privacy, thereby presenting a novel perspective on the progress of medical electronic devices.

REFERENCES

[1] J.-H. Syu, J. C.-W. Lin, G. Srivastava, and K. Yu, "A comprehensive survey on artificial intelligence empowered edge computing on consumer electronics," *IEEE Trans. Consum. Electron.*, vol. 69, no. 4, pp. 1023–1034, Nov. 2023.
[2] A. Yazdinejad, A. Dehghantanha, and G. Srivastava, "Ap2fl: Auditable privacy-preserving federated learning framework for electronics in healthcare," *IEEE Trans. Consum. Electron.*, vol. 70, no. 1, pp. 2527–2535, Feb. 2024.
[3] M. J. Molesky, "Communicating cybersecurity and privacy design attributes through privacy labeling of consumer electronic medical devices," *Front. Biomed. Devices*, vol. 84815, Apr. 2022, Art. no. V001T03A001.
[4] U. J. Muehlematter, P. Daniore, and K. N. Vokinger, "Approval of artificial intelligence and machine learning-based medical devices in the USA and Europe (2015–20): A comparative analysis," *Lancet Digit. Health*, vol. 3, no. 3, pp. e195–e203, 2021.
[5] B. Charamba et al., "Modeling the relationship between continuously measured glucose and electrocardiographic data in adults with type 1 diabetes mellitus," *Endocrinol. Diabetes Metab.*, vol. 4, no. 3, 2021, Art. no. e00263.
[6] B. Abhisheka, S. K. Biswas, B. Purkayastha, D. Das, and A. Escargueil, "Recent trend in medical imaging modalities and their applications in disease diagnosis: A review," *Multimedia Tools Appl.*, vol. 83, pp. 43035–43070, Apr. 2024.
[7] K. M. Boehm, P. Khosravi, R. Vanguri, J. Gao, and S. P. Shah, "Harnessing multimodal data integration to advance precision oncology," *Nat. Rev. Cancer*, vol. 22, no. 2, pp. 114–126, 2022.
[8] E. Luo, M. Z. A. Bhuiyan, G. Wang, M. A. Rahman, J. Wu, and M. Atiquzzaman, "PrivacyProtector: Privacy-protected patient data collection in IoT-based healthcare systems," *IEEE Commun. Mag.*, vol. 56, no. 2, pp. 163–168, Feb. 2018.
[9] J. Ficek, W. Wang, H. Chen, G. Dagne, and E. Daley, "Differential privacy in health research: A scoping review," *J. Am. Med. Inform. Assoc.*, vol. 28, no. 10, pp. 2269–2276, 2021.
[10] R. S. Antunes, C. André da Costa, A. Küderle, I. A. Yari, and B. Eskofier, "Federated learning for healthcare: Systematic review and architecture proposal," *ACM Trans. Intell. Syst. Technol.*, vol. 13, no. 4, pp. 1–23, 2022.
[11] A. Dosovitskiy et al., "An image is worth 16x16 words: Transformers for image recognition at scale," 2021, *arXiv:2010.11929*.
[12] S. Wang, X. Hu, and Q. Zhang, "HC-MAE: Hierarchical cross-attention masked autoencoder integrating histopathological images and multi-omics for cancer survival prediction," in *Proc. IEEE Int. Conf. Bioinformatics Biomed. (BIBM)*, 2023, pp. 642–647.
[13] K. Tomczak, P. Czerwinska, and M. Wiznerowicz, "The Cancer Genome Atlas (TCGA): An immeasurable source of knowledge," *Contemp. Oncol.*, vol. 19, no. 1A, pp. 68–77, 2015.

[14] A. Ullah, M. Azeem, H. Ashraf, A. A. Alaboudi, M. Humayun, and N. Jhanjhi, "Secure healthcare data aggregation and transmission in IoT-A survey," *IEEE Access*, vol. 9, pp. 16849–16865, 2021.
[15] A. Imakura and T. Sakurai, "Data collaboration analysis framework using centralization of individual intermediate representations for distributed data sets," *ASCE-ASME J. Risk Uncertainty Eng. Syst. Part A, Civil Eng.*, vol. 6, no. 2, 2020, Art. no. 04020018.
[16] J. J. Yang, J. Q. Li, and Y. Niu, "A hybrid solution for privacy preserving medical data sharing in the cloud environment," *Future Gener. Comput. Syst.*, vol. 43, pp. 74–86, Feb. 2015.
[17] S. Albarqouni, C. Baur, F. Achilles, V. Belagiannis, S. Demirci, and N. Navab, "AggNet: Deep learning from crowds for mitosis detection in breast cancer histology images," *IEEE Trans. Med. Imag.*, vol. 35, no. 5, pp. 1313–1321, May 2016.
[18] M. Y. Lu, D. F. K. Williamson, T. Y. Chen, R. J. Chen, M. Barbieri, and F. Mahmood, "Data-efficient and weakly supervised computational pathology on whole-slide images," *Nat. Biomed. Eng.*, vol. 5, no. 6, pp. 555–570, 2021.
[19] Y. Zhang et al., "Pseudo-data based self-supervised federated learning for classification of histopathological images," *IEEE Trans. Med. Imag.*, vol. 43, no. 3, pp. 902–915, Mar. 2024.
[20] O. Choudhury et al., "Differential privacy-enabled federated learning for sensitive health data," 2020, *arXiv:1910.02578*.
[21] C. Ding, A. Zhou, Y. Liu, R. N. Chang, C.-H. Hsu, and S. Wang, "A cloud-edge collaboration framework for cognitive service," *IEEE Trans. Cloud Comput.*, vol. 10, no. 3, pp. 1489–1499, Jul./Sep. 2020.
[22] S. Wang, S. Wang, and Z. Wang, "A survey on multi-omics-based cancer diagnosis using machine learning with the potential application in gastrointestinal cancer," *Front. Med.*, vol. 9, Jan. 2023, Art. no. 1109365.
[23] L. Schneider et al., "Integration of deep learning-based image analysis and genomic data in cancer pathology: A systematic review," *Eur. J. Cancer*, vol. 160, pp. 80–91, Jan. 2022.
[24] X. Wu, Y. Shi, M. Wang, and A. Li, "CAMR: Cross-aligned multimodal representation learning for cancer survival prediction," *Bioinformatics*, vol. 39, no. 1, 2023, Art. no. btad025.
[25] M. Y. Lu et al., "Federated learning for computational pathology on gigapixel whole slide images," *Med. Image Anal.*, vol. 76, Feb. 2022, Art. no. 102298.
[26] Q. Wang, M. He, L. Guo, and H. Chai, "AFEI: Adaptive optimized vertical federated learning for heterogeneous multi-omics data integration," *Brief. Bioinform.*, vol. 24, no. 5, 2023, Art. no. bbad269.
[27] C. Dwork and A. Roth, "The algorithmic foundations of differential privacy," *Found. Trends Theor. Comput. Sci.*, vol. 9, nos. 3–4, pp. 211–407, 2014.
[28] H. Huang, Q. Ye, and Y. Zhou, "6G-empowered offloading for realtime applications in multi-access edge computing," *IEEE Trans. Netw. Sci. Eng.*, vol. 10, no. 3, pp. 1311–1325, May/Jun. 2022.
[29] Y. Zhou, Q. Ye, and H. Huang, "DRL-based workload allocation for distributed coded machine learning," in *Proc. IEEE Int. Conf. Commun.*, 2023, pp. 3175–3180.
[30] R. Kumari, D. K. Sah, S. Gupta, K. Cengiz, and N. Ivkovic, "Advancing medical recommendations with federated learning on decentralized data: A roadmap for implementation," *IEEE Trans. Consum. Electron.*, vol. 70, no. 1, pp. 2666–2674, Feb. 2024.
[31] G. Srivastava, M. S. Mekala, M. S. Hajar, and H. Kalutarage, "C-NEST: Cloudlet based privacy preserving multidimensional data stream approach for healthcare electronics," *IEEE Trans. Consum. Electron.*, vol. 70, no. 1, pp. 1556–1565, Feb. 2024.

Suixue Wang received the B.S. degree in electronic and information engineering from Central South University, Changsha, China, and the M.S. degree in information and communication engineering from the Beijing Institute of Technology, Beijing, China. He is currently pursuing the Ph.D. degree in electronic and information engineering with Hainan University, Haikou, China. His research interests include deep learning and medical image processing.

Zhigao Zheng (Member, IEEE) is with Wuhan University. He is the Executive Committee Member of the Technical Committee on Distributed Computing & Systems and Embedded Systems of CCF. He published more than 20 peer-reviewed publications such as the IEEE TRANSACTIONS ON PARALLEL AND DISTRIBUTED SYSTEMS and the IEEE TRANSACTIONS ON COMPUTERS. He joins research projects from various governmental and industrial organizations, such as the National Science Foundation of China, the Ministry of Science and Technology, and the Ministry of Education. His current research interests focus on cloud computing, big data processing, and AI systems. He is the PC Member of several TOP conferences, such as TheWebConf (formally WWW) and NeurIPS, and the Vice PC Chair of CPSCom 2023. He is also an Editorial Board Member of some high quality journals, such as the IEEE TRANSACTIONS ON CONSUMER ELECTRONICS and *Mobile Networks and Applications*. He is a member of ACM and CCF.

Xinghong Wang received the B.S. degree in clinical medicine from Xinxiang Medical University, Xinxiang, China, in 2021. She is currently pursuing the M.S. degree in clinical laboratory diagnostics with the Hainan Medical College while undergoing standardized training with the First Affiliated Hospital of Hainan Medical College, Haikou, China. Her research interests include medical image processing and genomics data analysis.

Qingchen Zhang (Senior Member, IEEE) received the B.Eng. degree from Southwest University, China, and the Ph.D. degree from the Dalian University of Technology, China. He is currently a Professor with Hainan University, China. He has published over 20 papers in top international journals such as the IEEE TRANSACTIONS ON COMPUTERS, the IEEE TRANSACTIONS ON SERVICE COMPUTING, and the IEEE/ACM TRANSACTIONS ON COMPUTATIONAL BIOLOGY AND BIOINFORMATICS. His research has been supported by the National Natural Science Foundation of China and the Ministry of Science and Technology of the People's Republic of China. His research interests include big data, machine learning, and smart medicine.

Zhuo Liu is currently an Associate Professor with the Dalian Medical University, First Affiliated Hospital of Dalian Medical University. She has published 14 papers in international journals, and her research has been supported by the Liaoning Provincial Department of Science and Technology and the Dalian Municipal Science and Technology Bureau. Her research interests include smart medicine, big data, and machine learning.